ELSEVIER

Coordination Chemistry Reviews 226 (2002) 211–218

COORDINATION CHEMISTRY REVIEWS

www.elsevier.com/locate/ccr

Multi-electron reduction of CO_2 via Ru–CO_2, –C(O)OH, –CO, –CHO, and –CH_2OH species

Koji Tanaka [a,c,*], Dai Ooyama [b,c]

[a] *Institute for Molecular Science, Myodaiji, Okazaki 444-8585, Japan*
[b] *Faculty of Education, Fukushima University, Kanayagawa, Fukushima 960-1296, Japan*
[c] *CREST, Japan Science and Technology Corporation (JST), 4-1-8 Honmachi, Kawaguchi, Saitama 332-0012, Japan*

Received 23 April 2001; accepted 24 August 2001

Contents

Abstract

A series of $[Ru(bpy)_2(CO)L]^{n+}$ (L = CO_2, C(O)OH, CO, CHO, CH_2OH, CH_3, and $C(O)CH_3$; $n = 0$, 1, 2) were prepared and their molecular structures determined by X-ray analyses. These complexes are reasonable models of reaction intermediates in the multi-electron reduction of CO_2 catalyzed by metal complexes, since reductive cleavage of the Ru–L bonds of the complexes in protic media affords HCOOH, CO, HCHO, CH_3OH, and CH_4 as two-, four-, six- and eight-electron reduction products of CO_2. Thermodynamically, the free energy required in the reduction of CO_2 progressively decreases with an increase of the number of electrons participating in the reduction of CO_2. The Ru–L bond character of the series of $[Ru(bpy)_2(CO)L]^{n+}$ was assessed by the ν(Ru–L) bands and the Ru–L bond distances from the viewpoint of elucidation of a correlation between free energy changes in the multi-electron reduction of CO_2 catalyzed by metal complexes and the metal–carbon bond strength of each intermediate. The ruthenium–carbon bond distance of $[Ru(bpy)_2(CO)L]^{n+}$ largely depends on the hybrid orbital of the carbon atom bonded to ruthenium and lengthens in the order Ru–C_{sp} < Ru–C_{sp^2} < Ru–C_{sp^3}. An unusual shift of the ν(Ru–L) bands to higher wavenumber with decrease of the Ru–L bond distances was discussed in terms of σ- and π-character of the ruthenium–carbon bonds.

Keywords: Carbon dioxide; Ruthenium; Reduction of CO_2; Crystal structure; Carbonyl complex; Metal–carbon stretching vibration

1. Introduction

A striking characteristic of the reduction of carbon dioxide is that the equilibrium potentials (E vs. SCE, pH 7.0) progressively shift in a positive direction as the number of electrons participating in the reduction increases (Eqs. (1)–(6)). Multi-electron reduction of car-

* Corresponding author. Tel.: +81-564-55-7241; fax: +81-564-55-5245.
E-mail address: ktanaka@ims.ac.jp (K. Tanaka).

0010-8545/02/$ - see front matter
PII: S0010-8545(01)00434-9

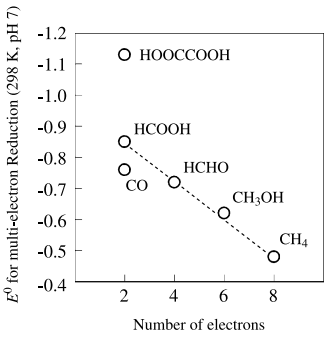

Fig. 1. Plots of $E°$ of reduction of CO_2 against number of electrons.

$$M—CO_2 \longrightarrow M—C(O)OH \longrightarrow M—CO \longrightarrow M—CHO \longrightarrow M—CH_2OH \longrightarrow M—CH_3$$

Scheme 1. Stepwise reduction of CO_2 on transition metal.

bon dioxide, therefore, is energetically favored compared with one- and two-electron reduction [1–13].

$$CO_2 + e^- \rightarrow CO_2^- \quad (E° = -2.14\ V) \tag{1}$$

$$CO_2 + 2e^- + 2H^+ \rightarrow HCOOH \quad (E° = -0.85\ V) \tag{2}$$

$$CO_2 + 2e^- + 2H^+ \rightarrow CO + H_2O \quad (E° = -0.76\ V) \tag{3}$$

$$CO_2 + 4e^- + 4H^+ \rightarrow H_2CO + H_2O \quad (E° = -0.72\ V) \tag{4}$$

$$CO_2 + 6e^- + 6H^+ \rightarrow CH_3OH + H_2O \quad (E° = -0.62\ V) \tag{5}$$

$$CO_2 + 8e^- + 8H^+ \rightarrow CH_4 + 2H_2O \quad (E° = -0.48\ V) \tag{6}$$

Plots of the equilibrium potential of the reactions in Eqs. (2)–(6) against the number of electrons suggest a strong correlation between them except for oxalic acid (Fig. 1). A variety of metal complexes have proven to work as homogeneous catalysts in the electrochemical reduction of carbon dioxide [14–40]. The first requisite for the homogeneous catalysts is that the redox potential of the metal complex lies in more negative region than the equilibrium potential of the reaction (Eqs. (2)–(6)). If one assumes that multi-electron reduction of carbon dioxide on metal complexes proceeds according to Scheme 1, two-, four-, six- and eight-electron reductions (Eqs. (2)–(6)) are explained in terms of reductive cleavages of metal–carbon bond of the reaction intermediates in protic media. A positive shift of the equilibrium potentials in Eqs. (2)–(6), therefore, may be associated with the metal–carbon bond strength of the M–C(O)OH, M–CO, M–CHO, M–CH_2OH, and M–CH_3 species. This article focuses on reactivity and the Ru–L bond character of a series of $[Ru(bpy)_2(CO)L]^{n+}$ (bpy = 2,2′-bipyridine, L = CO_2, C(O)OH, CO, CHO, CH_2OH, CH_3, and C(O)CH_3; $n = 0, 1, 2$) as intermediate models of the multi-electron reduction of carbon dioxide on ruthenium complexes.

2. Reduction of carbon dioxide under protic media

The dicationic ruthenium complex, $[Ru(bpy)_2(CO)_2]^{2+}$, is a representative homogeneous catalyst for electrochemical reduction of CO_2 in protic media [41–45]. In an aqueous solution, $[Ru(bpy)_2(CO)_2]^{2+}$ exists as an equilibrium mixture with $[Ru(bpy)_2(CO)(C(O)OH)]^+$ and $[Ru(bpy)_2(CO)(CO_2)]^0$ [46,47]. It is noteworthy that $[Ru(bpy)_2(CO)_2]^{2+}$ undergoes irreversible two-electron reduction at −1.0 V versus SCE to evolve CO with generation of $[Ru(bpy)_2(CO)]$, which complex has been shown to react with CO_2 to regenerate $[Ru(bpy)_2(CO)(CO_2)]^0$ (Scheme 2, path (a)) [48]. On the other hand, the reduction of $[Ru(bpy)_2(CO)_2]^{2+}$ with $NaBH_4$ in H_2O/CH_3OH produced $[Ru(bpy)_2(CO)(CHO)]^+$ as a yellow precipitate [49]. The similar reduction of $[Ru(bpy)_2(CO)_2]^{2+}$ with $NaBH_4$ in H_2O/CH_3CN in place of H_2O/CH_3OH afforded $[Ru(bpy)_2(CO)(CH_2OH)]^+$, since $[Ru(bpy)_2(CO)(CHO)]^+$ is soluble in H_2O/CH_3CN (Scheme 2, path (b)) [50]. The electrochemical reduction of $[Ru(bpy)_2(CO)(CH_2OH)]^+$ at −1.30 V in H_2O/CH_3CN generated CH_3OH and $[Ru(bpy)_2(CO)(CH_3CN)]^+$, but CH_4 was not produced at all [51]. In fact, numerous attempts to obtain $[Ru(bpy)_2(CO)(CH_3)]^+$ through $[Ru(bpy)_2(CO)(CH_2OH)]^+$ have been unsuccessful due to the preferential Ru–CH_2OH bond fission rather than $RuCH_2$–OH fission [49].

As mentioned above, $[Ru(bpy)_2(CO)(CO_2)]^{2+}$ is basically reduced up to $[Ru(bpy)_2(CO)(CH_2OH)]^+$ through $[Ru(bpy)_2(CO)_2]^{2+}$ (path (b) in Scheme 2), but neither $[Ru(bpy)_2(CO)(CHO)]^+$ nor $[Ru(bpy)_2(CO)(CH_2OH)]^+$ was generated in the electrochemical reduction of $[Ru(bpy)_2(CO)_2]^{2+}$. Note that $NaBH_4$ reacts with CO_2 to produce formic acid. Accordingly, even though

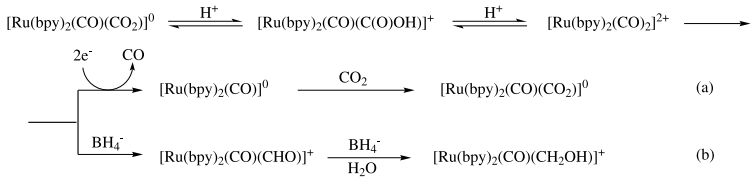

Scheme 2. Electrochemical (a) and chemical reduction (b) of $[Ru(bpy)_2(CO)_2]^{2+}$ equilibrated with $[Ru(bpy)_2(CO)(CO_2)]^0$ in aqueous solutions.

$[Ru(bpy)_2(CO)_2]^{2+}$ which exists as an equilibrium mixture with $[Ru(bpy)_2(CO)(CO_2)]^0$ is reduced to $[Ru(bpy)_2(CO)(CH_2OH)]^+$ by $NaBH_4$, reduction of CO_2 by $NaBH_4$ produces only HCOOH regardless of the presence of $[Ru(bpy)_2(CO)_2]^{2+}$. The lack of catalytic ability of $[Ru(bpy)_2(CO)_2]^{2+}$ towards four- and six-electron reduction of CO_2 apparently results from the reductive Ru–CO bond cleavage of the complex upon irreversible reduction at -1.0 V (path (a) in Scheme 2). On the other hand, $[Ru(bpy)(trpy)(CO)]^{2+}$ (trpy = 2,2′:6′,2″-terpyridine) undergoes one and two successive reversible one-electron reduction at room temperature and below 253 K, respectively (Eq. (7)) [50]. In CH_3CN/H_2O, $[Ru(bpy)(trpy)(CHO)]^+$ was formed in the reaction of $[Ru(bpy)(trpy)(CO)]^0$ with a proton at 253 K. As a result, the electrochemical reduction of CO_2 catalyzed by $[Ru(bpy)(trpy)(CO)]^{2+}$ at 253 K produced HCOOH, HCHO, CH_3OH, HOOCCHO, and $HOOCCH_2OH$ catalytically. The latter two were produced through an electrophilic attack of CO_2 on the ruthenium–carbon bond of $[Ru(bpy)(trpy)(CHO)]^+$ and $[Ru(bpy)(trpy)(CH_2OH)]^+$, respectively, under the electrolysis conditions.

$$[Ru(bpy)(trpy)(CO)]^{2+} \overset{e^-}{\rightleftarrows} [Ru(bpy)(trpy)(CO)]^{+} \overset{e^-}{\rightleftarrows} [Ru(bpy)(trpy)(CO)]^{0} \quad (7)$$

The catalytic activity of $[Ru(bpy)_2(CO)_2]^{2+}$ towards not only electrochemical but also photochemical reduction of CO_2 results from both reductive cleavage of the Ru–CO bond of $[Ru(bpy)_2(CO)_2]^{2+}$ upon irreversible reduction at -1.0 V and the subsequent adduct formation between the resultant $[Ru(bpy)_2(CO)]^0$ and CO_2 [52]. For example, $[Ru(bpy)_2(CO)_2]^{2+}$ worked as an efficient catalyst in the photochemical reduction of CO_2 using $[Ru(bpy)_3]^{2+}$ as a photosensitizer, in which $[Ru(bpy)_3]^+$ generated photochemically in the presence of sacrificial electron donors such as TEOA (triethanolamine) or BNAH (1-benzyl-1,4-dihydronicotinamide) functions as the electron donor to $[Ru(bpy)_2(CO)_2]^{2+}$ [53–57]. The catalytic activity of $[Ru(bpy)(trpy)(CO)]^{2+}$ toward the similar photochemical reduction of CO_2, on the other hand, was quite low compared with that of $[Ru(bpy)_2(CO)_2]^{2+}$, since the one-electron reduced form of $[Ru(bpy)(trpy)(CO)]^{2+}$ is stable and hardly produced CO and HCOOH at room temperature.

3. Characterization and structure analyses of the series of complexes of $[Ru(bpy)_2(CO)L]^{n+}$ ($L = CO_2$, C(O)OH, CO, CHO, CH_2OH, CH_3, and $C(O)CH_3$; $n = 0–2$)

We have carried out characterization of the series of $[Ru(bpy)_2(CO)L]^{n+}$ ($L = CO_2$, C(O)OH, CO, CHO, CH_2OH, CH_3 and $C(O)CH_3$) to elucidate the structural changes in the continuous reduction from CO_2 to CH_3 on ruthenium as shown in Scheme 1.

The preparation of $[Ru(bpy)_2(CO)_2]^{2+}$ was carried out in two different ways; one is the carbonylation of $[Ru(bpy)_2Cl_2]\cdot 2H_2O$ in an autoclave at 413 K under 20 atm of CO for 24 h [50], and the other is the reduction of $RuCl_3$ with formic acid and subsequent treatment of the resultant oligomeric $[RuCl_2(CO)_2]_n$ with 2,2′ bipyridine [58,59]. Colorless $[Ru(bpy)_2(CO)_2]^{2+}$ showed two strong ν(CO) bands at 2093 and 2039 cm^{-1}. The molecular structure (Fig. 2, $[Ru(bpy)_2(CO)(CO)]^{2+}$) reveals that the two carbonyl groups have essentially same parameters with respect to bond distances and angles. The short distances between carbon and oxygen atom (112 and 115 pm) support the triple bond character in both carbonyl moieties. The dicarbonyl complex was used as the precursor to the series of $[Ru(bpy)_2(CO)L]^{n+}$ ($L = CO_2$, C(O)OH, CHO, and CH_2OH).

A colorless H_2O/C_2H_5OH (1:1 v/v) solution of $[Ru(bpy)_2(CO)_2]^{2+}$ rapidly changed to yellow by addition of an equimolar amount of a methanolic $(C_4H_9)_4NOH$. From this solution, $[Ru(bpy)_2(CO)(C(O)OH)]PF_6$ was isolated as a yellow solid, but single crystals suitable for an X-ray structure analysis were not grown in the case of PF_6 salt probably due to protonation and deprotonation equilibrium of the amphoteric metallacarboxylic acid moiety [47]. This problem was overcome by use of trifluoromethane sulfonate as a counterion in the crystallization of $[Ru(bpy)_2(CO)(C(O)OH)]^+$ [60]. A monomeric structure of $[Ru(bpy)_2(CO)(C(O)OH)]^+$ is ascribed to the existence of a hydrate water molecule connecting two C(O)OH moieties. The molecular structure of $[Ru(bpy)_2(CO)(C(O)OH)]^+$ is shown in Fig. 2. The C=O, C–O bond distances (124.2 and 134.5 pm, respectively) and the O–C–O(H) bond angle (114°) of the complex are close to those of *trans*-$[Pt(C(O)OH)(C_6H_5)(P(C_2H_5)_3)_2]$ which exists as a dimeric form through two hydrogen bonds between the metallacarboxylate moieties [61]. On the other hand, the metallacarboxylate group of $[Ru(bpy)_2(CO)(C(O)OH)]^+$ binds to hydrated water (282.2 pm) which is also connected to triflate (276.9 pm) with another hydrogen bond. Furthermore, the hydrate water molecule is located in the neighborhood of the carbonyl oxygen of the metallacarboxylate group in another molecule of $[Ru(bpy)_2(CO)(C(O)OH)]^+$ (304.0 pm), suggesting a weak interaction between them.

A H_2O/C_2H_5OH (1:1 v/v) solution of $[Ru(bpy)_2(CO)_2]^{2+}$ turned to reddish yellow by addition of 2 equiv. of $(C_4H_9)_4NOH$. Slow evaporation of the reddish yellow solution gave red single crystals of $[Ru(bpy)_2(CO)(CO_2)]\cdot H_2O$ [62]. Mononuclear metal–CO_2 complexes reported so far either have an η^1- or η^2-CO_2 bonding mode [63–67]. On the basis of isotopic labeling studies, two bands at 1428 and 1242 cm^{-1} of

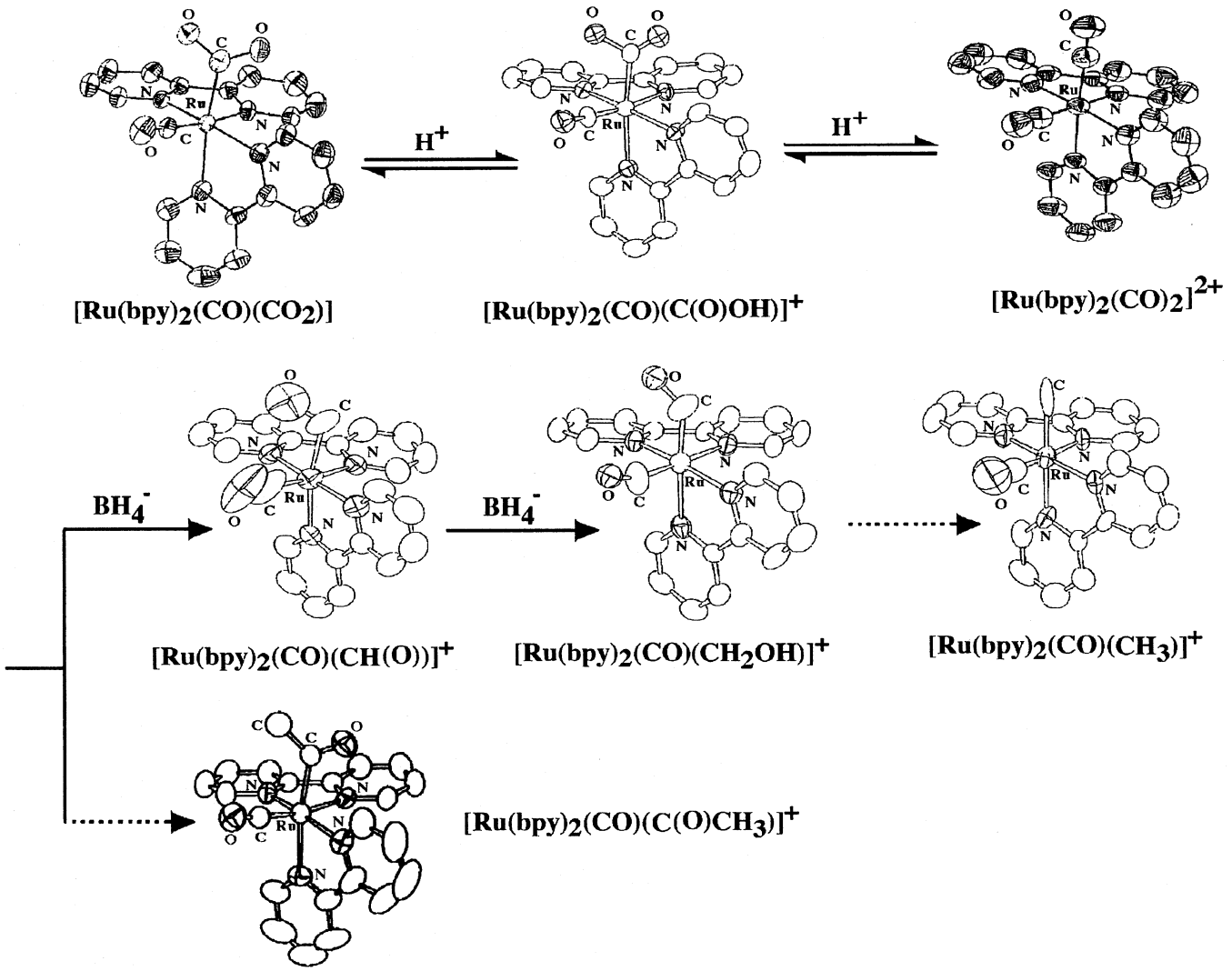

Fig. 2. X-ray analyses of crystal structures of $[Ru(bpy)_2(CO)L]^{n+}$ (L = CO_2, C(O)OH, CO, CHO, CH_2OH, CH_3, and $C(O)CH_3$; $n = 0$, 1, 2).

$[Ru(bpy)_2(CO)(CO_2)] \cdot 3H_2O$ were assigned to $\nu_{asym}(CO_2)$ and $\nu_{sym}(CO_2)$ bands, respectively, indicating the existence of the η^1-CO_2 group in the complex. This result was supported by the X-ray structure analysis. The ORTEP of $[Ru(bpy)_2(CO)(CO_2)]$ is depicted in Fig. 2 ($[Ru(bpy)_2(CO)(CO_2)]$). Red crystals of $[Ru(bpy)_2(CO)(CO_2)] \cdot 3H_2O$ contain three-dimensional hydrogen binding networks among two oxygen atoms of the η^1-CO_2 ligand and three hydrate molecules, which must assist electron flow to the CO_2 group from ruthenium and stabilize the Ru–CO_2 bond. The two non-equivalent C–O bond distances (125 and 128 pm) of the η^1-CO_2 group are ascribed to the differences in the number of hydrogen bonds between the two oxygen atoms and hydrate water molecules. The Ru–CO_2 bond distance (206 pm) is close to that of $[RhCl(diars)_2(\eta^1$-$CO_2)]$ (diars = *o*-phenylenebis(dimethylarsine)) (205 pm) [68] but longer than that of Co(Pr–salen)(η^1-CO_2)K^+ (salen = *N*,*N*′-ethylenebis(salicylideniminato)) (199 pm) [69]. The O–C–O bond angle of the complex is 121° and narrower than that of Co–CO_2 (135°) and Rh–CO_2 (126°). Taking into account that the O–C–O angle of CO_2^- is 135° [4], the Ru–CO_2 bond is formulated as Ru(II)–CO_2^{2-} rather than Ru(0)–CO_2. As is distinct from other η^1-CO_2 metal complexes, $[Ru(bpy)_2(CO)(CO_2)] \cdot 3H_2O$ is very stable thermally and does not dissociate to release CO_2 in H_2O even at 353 K. The unusual stability of $[Ru(bpy)_2(CO)(CO_2)]$ in the η^1-CO_2 metal complexes is associated with hydrogen bonding between the η^1-CO_2 group and three H_2O molecules, which would effectively reduce the high electron density of the CO_2 group.

Some metal–carbonyl complexes are reduced stepwise to formyl, hydroxymethyl, and methyl derivatives by hydride donors such as $NaBH_4$ and metal-hydrides [70–72]. In fact, a colorless $CH_3OH/(CH_3)_2CO$ solution (2:1 v/v) of $[Ru(bpy)_2(CO)_2]^{2+}$ rapidly changed to yellow in color by an addition of aqueous $NaBH_4$ (1.5 equiv.) at 253 K, and yellow single crystals of $[Ru(bpy)_2(CO)(CHO)]PF_6$ gradually appeared after ad-

dition of diethyl ether to the solution at the same temperature [73]. In contrast to the thermal stability of $[Ru(bpy)_2(CO)(CO_2)]$ in CH_3OH and H_2O, $[Ru(bpy)_2(CO)(CHO)]^+$ decomposed above 253 K in solution. For example, thermal decomposition of $[Ru(bpy)_2(CO)(CHO)]^+$ in CH_3OH at 273 K gave $[Ru(bpy)_2(CO)(C(O)OCH_3)]^+$ and H_2 molecule (Eq. (8)). Similar thermolysis of $[Ru(bpy)_2(CO)(CHO)]^+$ in CO_2-saturated CH_3CN at 273 K produced $HCOO^-$ and regenerated $[Ru(bpy)_2(CO)_2]^{2+}$ (Eq. (9)).

$$[Ru(bpy)_2(CO)(CHO)]^+ + CH_3OH \rightarrow [Ru(bpy)_2(CO)(C(O)OCH_3)]^+ + H_2 \quad (8)$$

$$[Ru(bpy)_2(CO)(CHO)]^+ + CO_2 \rightarrow [Ru(bpy)_2(CO)_2]^{2+} + HCOO^- \quad (9)$$

The X-ray analysis of $[Ru(bpy)_2(CO)(CHO)]^+$ revealed the molecular structure of the complex with a *cis*-orientation of the Ru–CO and Ru–CHO moieties (Fig. 2, $[Ru(bpy)_2(CO)(CHO)]^+$). The bond distances and angles of the Ru–CO and Ru–CHO groups, however, could not be determined due to disorder of the two groups in the crystal structure at 243 K. The ambiguity of the local structures due to disorder of the Ru–CO and Ru–CHO groups in the solid state was not improved in the X-ray measurement conducted even at 123 K.

An aqueous solution of $NaBH_4$ reacted with $[Ru(bpy)_2(CO)_2]^{2+}$ in CH_3CN/H_2O at 253 K for 30 min, and then the mixture was further stirred at room temperature for 4 h. Gas chromatography analyses of the resulting solution revealed the formation of CH_3OH. The yield of CH_3OH increased with increasing amount of BH_4^- used. Especially, the carbonyl ligand of $[Ru(bpy)(trpy)(CO)]^{2+}$ was quantitatively reduced to CH_3OH by treatment with 4 equiv. of $NaBH_4$ while the carbonyl ligand of $[Ru(bpy)_2(CO)_2]^{2+}$ was reduced to CH_3OH in a 10% yield under the same reaction conditions (Fig. 3) [50]. Thus, the carbonyl ligand of $[Ru(bpy)(trpy)(CO)]^{2+}$ is much more subject to reduction than that of $[Ru(bpy)_2(CO)_2]^{2+}$. Yellow

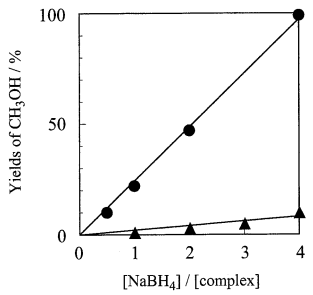

Fig. 3. Yields of CH_3OH in the reaction of $[Ru(bpy)_2(CO)_2]^{2+}$ (▲) and $[Ru(bpy)(trpy)(CO)]^{2+}$ (●) with various amounts of $NaBH_4$ in CH_3CN/H_2O.

$[Ru(bpy)_2(CO)(CH_2OH)]^+$ was isolated as a precursor to CH_3OH in the reaction of $[Ru(bpy)_2(CO)_2]^{2+}$ with 1.5 equiv. of BH_4^-, but $[Ru(bpy)(trpy)(CH_2OH)]^+$ was not confirmed due to the high reactivity of $[Ru(bpy)(trpy)(CH_2OH)]^+$ toward protons. The X-ray structure analysis of $[Ru(bpy)_2(CO)(CH_2OH)]^+$ revealed the octahedral coordination geometry with terminal carbonyl and hydroxymethyl ligands as shown in Fig. 2. From the detailed analyses, the oxygen atom of the hydroxymethyl group was disordered over two sites to give two isomers [74]. In harmony with this, the Raman spectra of the complex showed two $\nu(Ru–CH_2OH)$ bands derived from these isomers in the solid state.

The methyl complex would work as the precursor to methane as the final product in the multi-electron reduction of CO_2. However, we could not cleave the $RuCH_2–OH$ bond of $[Ru(bpy)_2(CO)(CH_2OH)]^+$ selectively without accompanying $Ru–CH_2OH$ bond fission. So, $[Ru(bpy)_2(CO)(CH_3)]^+$ was prepared by the reaction of $[Ru(bpy)_2(OH_2)_2]^{2+}$ with trimethylsilyl acetylene in H_2O [73,75]. $[Ru(bpy)_2(CO)(CH_3)]^+$ was stable even in H_2O despite having a metal–alkyl bond in its coordination sphere. The crystal structure of $[Ru(bpy)_2(CO)(CH_3)]^+$ is depicted in Fig. 2. The $[Ru(bpy)_2(CO)(CH_3)]^+$ cation also has the expected octahedral coordination geometry and two bidentate bipyridine ligands are situated in a *cis* position with each other. The Ru–C–O (carbonyl) bond angles are essentially linear (174°), and Ru–C and C–O bond distances (177 and 115 pm, respectively) are also typical in other carbonylruthenium(II) complexes [50,60, 62,73,74].

As mentioned earlier, disorder of the Ru–CO and Ru–CHO bonds in the crystal structure of the $[Ru(bpy)_2(CO)(CHO)]^+$ caused a serious problem in determining accurately the bond parameters of the two groups. The disorder of the two groups in the solid state of $[Ru(bpy)_2(CO)(CHO)]^+$ probably results from small differences in the sizes between CO and CHO moieties. Therefore, $[Ru(bpy)_2(CO)(C(O)CH_3)]^+$ was synthesized in place of the formyl complex to obtain accurate bond parameters of the acyl moiety. The reaction of $[Ru(bpy)_2(CO)_2]^{2+}$ with CH_3Li and CH_3MgI resulted in irreversible reduction with evolution of CO due to the intermolecular electron transfer from these alkylation agents to the dicarbonyl complex. Accordingly, $[Ru(bpy)_2(CO)(C(O)CH_3)]^+$ was prepared by the reaction of $[Ru(bpy)_2(CO_3)]$ with propiolic acid in H_2O [73,75]. This complex was stable in general organic solvents such as CH_3CN, CH_2Cl_2, and CH_3OH. The infrared spectra of $[Ru(bpy)_2(CO)(C(O)CH_3)]^+$ showed the $\nu(CO)$ and $\nu(C=O)$ bands at 1939 and 1607 cm^{-1}, respectively, and the ^{13}C-NMR spectra demonstrated the characteristic signals at δ 203 (CO) and 263 (C=O). These data are close to those of $[Ru(bpy)_2(CO)-$

Table 1
Relevant vibrational bands and bond parameters for $[Ru(bpy)_2(CO)L]^{n+}$ (L = CO_2, C(O)OH, CO, CHO, CH_2OH, CH_3, and $C(O)CH_3$; $n = 0$, 1, 2)

L	ν(CO)/cm^{-1}	ν(Ru–L)/cm^{-1}	d(C–O)/pm	d(Ru–C)/pm	∠(Ru–C–O)/°	d(Ru–L)/pm
CO_2	1948	520	115	181	179	206
C(O)OH	1974	511	117	179	177	200
CO	2076 [a]	444 [a]	113 [a]	189 [a]	177 [a]	189 [a]
CHO	1950	519	112 [b]	188 [b]	165 [b]	188[b]
CH_2OH	1929 [c]	541 [c]	111	185	170	219
CH_3	1921	529	115	177	174	221
$C(O)CH_3$	1939	511	115	184	176	204

[a] The mean of the two carbonyl groups.
[b] The mean of the disordered CO and CHO groups.
[c] The mean of the two isomers.

$(CHO)]^+$ [49], suggesting that the electron density of the acetyl group is comparable to that of the formyl one. Thus, $[Ru(bpy)_2(CO)(C(O)CH_3)]^+$ is a suitable model for $[Ru(bpy)_2(CO)(CHO)]^+$ from the similarities of the infrared and NMR spectra. The crystal structure of $[Ru(bpy)_2(CO)(C(O)CH_3)]^+$ (Fig. 2) confirms the octahedral coordination geometry. The structural parameters of $[Ru(bpy)_2(CO)(C(O)CH_3)]^+$ were compared with the corresponding formyl complex, and no significant difference was observed in the $Ru(bpy)_2$ moieties. The sum of three bond angles around the acetyl carbon (Ru–C–O, Ru–C–C(H_3), and O–C–C(H_3)) is 360°, indicating the sp^2 hybrid orbital of the acetyl carbon atom in analogy with other two complexes (L = CO_2 and C(O)OH).

4. Comparison in the Ru–C bond character in the series of complexes of $[Ru(bpy)_2(CO)L]^{n+}$ (L = CO_2, C(O)OH, CO, CHO, CH_2OH, CH_3, and $C(O)CH_3$; $n = 0$–2)

Vibrational spectral data on organometallic compounds have been well documented and elucidated the presence of various coupling between metal–carbon stretching modes [76–80]. On the other hand, ν(CO) often provides valuable information about the structure and bonding of carbonyl complexes, since ν(CO) is generally free from coupling with other modes [81]. The ν(CO) bands in the series of $[Ru(bpy)_2(CO)L]^{n+}$ (L = CO_2, C(O)OH, CO, CHO, CH_2OH, CH_3, and $C(O)CH_3$; $n = 0$–2) appeared in the range of 2076 (L = CO) to 1921 cm^{-1} (L = CH_3) in agreement with the terminal carbonyl in these complexes [81]. The order of shift of the ν(CO) bands to lower wavenumber (L = CO < C(O)OH < CHO < CH_2OH < $C(O)CH_3$ < CH_3) is reasonably correlated with the electron-donating ability of the substituent L (Table 1).

The tendency indicates that the electron donor character of the sp^3 carbon in the ligand L to ruthenium is stronger than that of sp^2 and sp carbon. We also assessed the Ru–L bond characters of $[Ru(bpy)_2(CO)L]^{n+}$ by means of Raman spectra. Metal–carbon stretching modes usually emerge in the range of 1000–200 cm^{-1} [82]. Table 1 also summarizes ruthenium–carbon stretching bands (ν(Ru–L)) determined from Raman spectra using isotope labeling studies. The Raman spectra of $[Ru(bpy)_2(CO)L]^{n+}$ revealed that $\nu(Ru–C_{sp^3})$, $\nu(Ru–C_{sp^2})$, and $\nu(Ru–C_{sp})$ bands of the complexes reside in the range of 525–540 cm^{-1} (L = CH_3 and CH_2OH), 510–520 cm^{-1} (L = CO_2, C(O)OH, CHO, $C(O)CH_3$), and at 444 cm^{-1} (L = CO), respectively (Table 1). The correlation between ν(CO) and ν(Ru–L) in Fig. 4, therefore, is explained by an enhancement of σ- and π-bonding character of the Ru–CO and Ru–L bonds, respectively, with increasing electron-donating ability of the L ligands.

The crystal structures of all these complexes have been determined by X-ray analyses. The C–O, Ru–C, and Ru–L bond distances, and Ru–C–O bond angles are summarized in Table 1. The Ru–C (carbonyl) and C–O bond distances of $[Ru(bpy)_2(CO)L]^{n+}$ are in the range of 177–189 pm and 111–117 pm, respectively, in the series complexes. Further, Ru–C–O bond angles are essentially linear (170–179°). Thus, the Ru–CO bond parameters of the complexes are very close to each

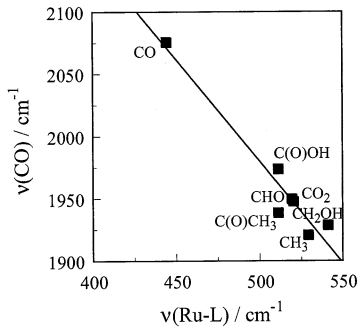

Fig. 4. Relationship between ν(CO) and ν(Ru–L) bands of $[Ru(bpy)_2(CO)L]^{n+}$ (L = CO_2, C(O)OH, CO, CHO, CH_2OH, CH_3, and $C(O)CH_3$).

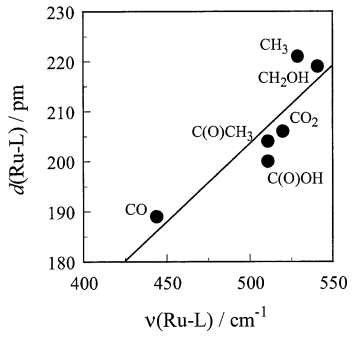

Fig. 5. Relationship between Ru–L bond distances (d(Ru–L)) and ν(Ru–L) bands of $[Ru(bpy)_2(CO)L]^{n+}$ (L = CO_2, C(O)OH, CO, CH_2OH, CH_3, and $C(O)CH_3$).

other. On the other hand, the differences in the Ru–L bond distances in the series of $[Ru(bpy)_2(CO)L]^{n+}$ lie apparently beyond the range of 10% (from 189 to 221 pm)! The bond distances in the order of $Ru–C_{sp} < Ru–C_{sp^2} < Ru–C_{sp^3}$ reveal the shortening of the ruthenium–carbon (L) bond distance as the $d\pi–p\pi$ interaction increases between the ruthenium and carbon atoms. A plot of the Ru–L bond distances (d(Ru–L)) against ν(Ru–L) suggests a strong correlation between them (Fig. 5). Unusual shifts of the ν(Ru–L) bands of $[Ru(bpy)_2(CO)L]^{n+}$ to higher wavenumber with elongation of the Ru–L bond distances would be associated with σ- and π-bond character of the bonds.

The potential energy of a simple vibration of two nuclei in a diatomic molecule is simply given by Eq. (10), where V is the potential energy, K is the force constant for the vibration, and q is the displacement from its equilibrium position [83]. The frequency of the vibration in a diatomic molecule (ν) is proportional to the square root of K as expressed by Eq. (11) (μ = reduced mass).

$$V = 1/2Kq^2 \tag{10}$$

$$\nu = 1/2\pi(K/\mu)^{1/2} \tag{11}$$

The force constant is a measure of the curvature of the potential well near the equilibrium position (Eq. (12)).

$$K = (d^2V/dq^2)_{q\to 0} \tag{12}$$

Thus, a large force constant means sharp curvature of the potential well near the bottom, but does not necessarily indicate a deep potential well. Coupling of the ν(Ru–L) band and other vibrational modes in the series of $[Ru(bpy)_2(CO)L]^{n+}$ would be not so different due to the similarity of their molecular structures. The order of $Ru–C_{sp} < Ru–C_{sp^2} < Ru–C_{sp^3}$ of the ν(Ru–L) band in Fig. 5, therefore, is the same as that of the force constant of the Ru–L bond. The curvature of the potential well near equilibrium positions of the $Ru–C_{sp}$ bond (π-bond) must be milder than that of the $Ru–C_{sp^3}$ one (σ-bond). This result also indicates flexibility and stiffness in the π- and σ-bond, respectively, in the stretching vibrations. Thus, the unusual relationship between d(Ru–L) and ν(Ru–L) in Fig. 5 apparently results from the drastic change of the Ru–L bond character from $Ru–C_{sp}$ to $Ru–C_{sp^3}$ in the series of $[Ru(bpy)_2(CO)L]^{n+}$ (L = CO_2, C(O)OH, CO, CHO, CH_2OH, CH_3, and $C(O)CH_3$; n = 0–2).

5. Conclusions

A large number of electro and photochemical reduction reactions of CO_2 catalyzed by metal complexes have been reported so far. One of the noticeable characteristics of CO_2 is a decrease in free energy change with an increase in the number of electrons involved in the reduction of CO_2. Despite the thermodynamic trend, the products in the reduction of CO_2 mediated with metal complexes have been limited to CO and/or HCOOH. Elucidation of the reaction mechanism and the active species of the CO_2 reduction would develop new methodology for multi-electron reduction of CO_2 by homogeneous catalysts. Taking into account that the series of $[Ru(bpy)_2(CO)L]^{2+}$ (L = CO_2, C(O)OH, CO, CHO, CH_2OH, CH_3 and $C(O)CH_3$) are reasonable models of reaction intermediates in multi-electron reduction of CO_2 on Ru, the difficulty of four-electron reduction of CO_2 is considered to result from both reductive Ru–CO bond cleavage and thermal lability of the Ru–CHO bond. Reduction of metal–CO bonds without accompanying bond cleavage in protic media, therefore, may lead to a breakthrough in utilization of CO_2 as a C1 resource.

References

[1] A.J. Bard (Ed.), Encyclopedia of Electrochemistry of the Elements, vol. 7, Dekker, New York, 1976.
[2] N. Sutin, C. Creustz, Adv. Chem. Ser. 168 (1978) 1.
[3] R. Ziessel, Nouv. J. Chim. 7 (1983) 613.
[4] C. Amatore, J.-M. Savéant, J. Am. Chem. Soc. 103 (1986) 5021.
[5] J. Hawecker, J.-M. Lehn, R. Ziessel, Helv. Chim. Acta 69 (1986) 1990.
[6] Y. Hori, A. Murata, R. Takahashi, S. Suzuki, J. Am. Chem. Soc. 109 (1987) 5022.
[7] J.P. Collin, J.P. Sauvage, Coord. Chem. Rev. 93 (1989) 245.
[8] I. Willner, B. Willner, Top. Curr. Chem. 159 (1991) 153.
[9] M. Hammouche, D. Lexa, M. Momenteau, J.-M. Savéant, J. Am. Chem. Soc. 113 (1991) 8455.
[10] Y. Hori, A. Murata, R. Takahashi, S. Suzuki, J. Chem. Soc. Chem. Commun. (1992) 767.
[11] B.P. Sullivan, K. Krist, H.E. Guard (Eds.), Electrochemical and Electrocatalytic Reduction of Carbon Dioxide, Elsevier, Amsterdam, 1993.
[12] W. Leitner, Angew. Chem. Int. Ed. Engl. 34 (1995) 2207.
[13] J. Costamagna, G. Ferraudi, J. Canales, J. Vargas, Coord. Chem. Rev. 148 (1996) 221.

[14] M. Tezuka, T. Yajima, A. Tsuchida, Y. Matsumoto, Y. Uchida, M. Hidai, J. Am. Chem. Soc. 104 (1982) 6834.
[15] S. Slater, J.H. Wagenknecht, J. Am. Chem. Soc. 106 (1984) 5367.
[16] J. Hawecker, J.-M. Lehn, R. Ziessel, J. Chem. Soc. Chem. Commun. (1984) 328.
[17] C.M. Bolinger, B.P. Sullivan, D. Conrad, J.A. Gilbert, N. Story, T.J. Meyer, J. Chem. Soc. Chem. Commun. (1985) 796.
[18] B.P. Sullivan, C.M. Bolinger, D. Conrad, W.J. Vining, T.J. Meyer, J. Chem. Soc. Chem. Commun. (1985) 1414.
[19] M. Nakazawa, Y. Mizobe, Y. Matsumoto, Y. Uchida, M. Tezuka, M. Hidai, Bull. Chem. Soc. Jpn. 59 (1986) 809.
[20] C.R. Cabrera, H.D. Abruna, J. Electroanal. Chem. Intrafacial Electrochem. 209 (1986) 101.
[21] M. Beley, J.-P. Collin, R. Ruppert, J.-P. Sauvage, J. Am. Chem. Soc. 106 (1986) 7461.
[22] M.R.M. Bruce, E. MeGehee, B.P. Sullivan, H. Thorp, T.R. O'Toole, A. Downard, T.J. Meyer, Organometallics 7 (1988) 238.
[23] C.M. Bolinger, N. Story, B.P. Sullivan, T.J. Meyer, Inorg. Chem. 27 (1988) 4582.
[24] S. Cosnier, A. Deronzier, J.-C. Moutet, J. Mol. Catal. 45 (1988) 381.
[25] K. Tanaka, T. Matsui, T. Tanaka, J. Am. Chem. Soc. 111 (1989) 3765.
[26] A. Szymaszek, F.P. Pruchnik, J. Organomet. Chem. 376 (1989) 133.
[27] H.C. Hurrell, A.L. Mogstad, D.A. Usifer, K.T. Potts, H.D. Abruna, Inorg. Chem. 28 (1989) 1080.
[28] T.R. O'Toole, B.P. Sullivan, M.R.M. Bruce, L.D. Margerum, R.W. Murray, T.J. Meyer, J. Electroanal. Chem. Intrafacial Electrochem. 259 (1989) 217.
[29] T. Tomohiro, K. Uoto, H.Y. Okuno, J. Chem. Soc. Chem. Commun. (1990) 194.
[30] S. Rasmussen, M.M. Richter, E. Yi, H. Place, K.J. Brewer, Inorg. Chem. 29 (1990) 3926.
[31] S. Sasaki, J. Am. Chem. Soc. 112 (1990) 7813.
[32] J.R. Pugh, M.R.M. Bruce, B.P. Sullivan, T.J. Meyer, Inorg. Chem. 30 (1991) 86.
[33] M.R.M. Bruce, E. MeGehee, B.P. Sullivan, H.H. Thorp, T.R. O'Toole, A. Downard, J.R. Pugh, T.J. Meyer, Inorg. Chem. 31 (1992) 4864.
[34] P. Christensen, A. Hamnett, A.V.G. Muir, J.A. Timney, J. Chem. Soc. Dalton Trans. (1992) 1455.
[35] S. Sasaki, J. Am. Chem. Soc. 114 (1992) 2055.
[36] T. Yoshida, K. Tsutsumida, S. Teratani, K. Yasufuku, M. Kaneko, J. Chem. Soc. Chem. Commun. (1993) 631.
[37] T. Yoshida, T. Iida, T. Shirasagi, R.-J. Lin, M. Kaneko, J. Electroanal. Chem. Intrafacial Electrochem. 344 (1993) 355.
[38] M.-N. Collomb-Dunand-Sauthier, A. Deronzier, R. Ziessel, Inorg. Chem. 33 (1994) 2961.
[39] E. Fujita, J. Haff, R. Sanzenbacher, H. Elias, Inorg. Chem. 33 (1994) 4627.
[40] F.P.A. Johnson, M.W. George, F. Hartl, J.J. Turner, Organometallics 15 (1996) 3374.
[41] H. Ishida, H. Tanaka, K. Tanaka, J. Chem. Soc. Chem. Commun. (1987) 131.
[42] H. Ishida, K. Tanaka, T. Tanaka, Organometallics 6 (1987) 181.
[43] H. Ishida, H. Tanaka, K. Tanaka, T. Tanaka, Chem. Lett. (1987) 597.
[44] H. Ishida, K. Fujiki, T. Ohba, K. Ohkubo, K. Tanaka, T. Tanaka, J. Chem. Soc. Dalton Trans. (1990) 2155.
[45] S. Chardon-Noblat, M.-N. Collomb-Dunand-Sauthier, A. Deronzier, R. Ziessel, D. Zsoldos, Inorg. Chem. 33 (1994) 4410.
[46] K. Tanaka, M. Morimoto, T. Tanaka, Chem. Lett. (1983) 901.
[47] H. Ishida, K. Tanaka, M. Morimoto, T. Tanaka, Organometallics 5 (1986) 724.
[48] E. Fujita, M. Chou, K. Tanaka, Appl. Organomet. Chem. 14 (2000) 844.
[49] K. Toyohara, H. Nagao, T. Mizukawa, K. Tanaka, Inorg. Chem. 34 (1995) 5399.
[50] H. Nagao, T. Mizukawa, K. Tanaka, Inorg. Chem. 33 (1994) 3415.
[51] K. Toyohara, K. Tanaka, unpublished result.
[52] E. Fujita, Coord. Chem. Rev. 185–186 (1999) 373.
[53] H. Ishida, K. Tanaka, T. Tanaka, Chem. Lett. (1987) 1035.
[54] H. Ishida, K. Tanaka, T. Tanaka, Inorg. Chem. 26 (1987) 553.
[55] H. Ishida, K. Tanaka, T. Tanaka, Chem. Lett. (1988) 339.
[56] H. Ishida, T. Terada, K. Tanaka, T. Tanaka, Inorg. Chem. 29 (1990) 905.
[57] J.-M. Lehn, R. Ziessel, J. Organomet. Chem. 382 (1990) 157.
[58] P.A. Anderson, G.B. Deacon, K.H. Haarmann, F.R. Keene, T.J. Meyer, D.A. Reitsma, B.W. Skelton, G.F. Strouse, N.C. Thomas, J.A. Tredway, A.H. White, Inorg. Chem. 34 (1995) 6145.
[59] J.A. Tredway, T.J. Meyer, Inorg. Chem. 38 (1999) 2267.
[60] K. Toyohara, H. Nagao, T. Adachi, T. Yoshida, K. Tanaka, Chem. Lett. (1996) 27.
[61] M. Bennett, A. Rokicki, Organometallics 4 (1985) 180.
[62] H. Tanaka, B.-C. Tzeng, H. Nagao, S.-M. Peng, K. Tanaka, Inorg. Chem. 32 (1993) 1508.
[63] K. Tanaka, Adv. Inorg. Chem. 43 (1995) 409.
[64] K. Tanaka, K. Tsuge, Trends Inorg. Chem. 4 (1996) 145.
[65] D.H. Gibson, Chem. Rev. 96 (1996) 2063.
[66] K. Tanaka, Bull. Chem. Soc. Jpn. 71 (1998) 17.
[67] D.H. Gibson, Coord. Chem. Rev. 185–186 (1999) 335.
[68] J.C. Calabrese, T. Herskovitz, J.B. Kinney, J. Am. Chem. Soc. 105 (1983) 5914.
[69] G. Fachinetti, C. Floriani, P.F. Zanazzi, J. Am. Chem. Soc. 100 (1978) 7405.
[70] P.M. Treichel, R.L. Schubhin, Inorg. Chem. 6 (1967) 1328.
[71] C. Lapinte, D. Astruc, J. Chem. Soc. Chem. Commun. (1983) 430.
[72] C. Lapinte, D. Catheline, D. Astruc, Organometallics 7 (1988) 1683.
[73] D. Ooyama, T. Tomon, K. Tsuge, K. Tanaka, J. Organomet. Chem. 619 (2001) 299.
[74] K. Toyohara, K. Tsuge, K. Tanaka, Organometallics 14 (1995) 5099.
[75] C. Mountassir, T.B. Hadda, H. Le Bozec, J. Organomet. Chem. 388 (1990) C13.
[76] R. Caballol, M.E. Sanchez, J.C. Barthelat, J. Phys. Chem. 91 (1987) 1328.
[77] C. Jegat, M. Fouassier, J. Mascetti, Inorg. Chem. 30 (1991) 1521.
[78] C. Jegat, M. Fouassier, M. Tranquille, J. Mascetti, Inorg. Chem. 30 (1991) 1529.
[79] C. Jegat, M. Fouassier, M. Tranquille, J. Mascetti, I. Tommasi, M. Aresta, F. Ingold, A. Dedieu, Inorg. Chem. 32 (1993) 1279.
[80] G. Davidson (Ed.), Spectroscopic Properties of Inorganic and Organometallic Compounds, vol. 30, The Royal Society of Chemistry, London, 1997.
[81] K. Nakamoto, Infrared and Raman Spectra of Inorganic and Coordination Compounds, 4th ed., Wiley, New York, 1986, pp. 291–294.
[82] F.R. Hartley, S. Patai (Eds.), The Chemistry of the Metal–Carbon Bond, vol. 1, Wiley, Chichester, 1982 (and references therein).
[83] Ref. [81], pp. 9–12.